catalysts

MDPI

Article

Thermodynamic and Kinetic Investigation on *Aspergillus ficuum* Tannase Immobilized in Calcium Alginate Beads and Magnetic Nanoparticles

Jônatas de Carvalho-Silva [1,†], Milena Fernandes da Silva [2,†], Juliana Silva de Lima [3,†], Tatiana Souza Porto [4], Luiz Bezerra de Carvalho, Jr. [3] and Attilio Converti [5,*]

1 Northeast Biotechnology Network, Federal University of the Agreste of Pernambuco (UFAPE), Av. Bom Pastor, s/n–Boa Vista, Garanhuns 55292-270, PE, Brazil; jonatas_carvalho.jcs@hotmail.com
2 Northeast Strategic Technologies Center (CETENE), Ministry of Science, Technology and Innovation (MCTI), Av. Prof. Luis Freire, 01, Cidade Universitária, Recife 50740-545, PE, Brazil; milena.silva@cetene.gov.br
3 Laboratory of Immunopathology Keizo Asami (LIKA), Department of Biochemistry, Federal University of Pernambuco, Av. Prof. Moraes Rego, Recife 50670-901, PE, Brazil; ju_db_08@hotmail.com (J.S.d.L.); lbcj.br@gmail.com (L.B.d.C.J.)
4 Department of Animal Morphology and Physiology, Federal Rural University of Pernambuco (UFRPE), Rua Dom Manuel de Medeiros, s/n, Dois Irmãos, Recife 52171-900, PE, Brazil; tatiana.porto@ufrpe.br
5 Department of Civil, Chemical and Environmental Engineering, University of Genoa (UNIGE), Pole of Chemical Engineering, via Opera Pia 15, 16145 Genoa, Italy
* Correspondence: converti@unige.it
† These authors contributed equally to this work.

Abstract: Tannase from *Aspergillus ficuum* was immobilized by two different techniques for comparison of kinetic and thermodynamic parameters. Tannase was either entrapped in calcium alginate beads or covalently-immobilized onto magnetic diatomaceous earth nanoparticles. When immobilized on nanoparticles, tannase exhibited lower activation energy (15.1 kJ/mol) than when immobilized in alginate beads (31.3 kJ/mol). Surprisingly, the thermal treatment had a positive effect on tannase entrapped in alginate beads since the enzyme became more solvent exposed due to matrix leaching. Accordingly, the proposed mathematical model revealed a two-step inactivation process. In the former step the activity increased leading to activation energies of additional activity of 3.1 and 26.8 kJ/mol at 20–50 °C and 50–70 °C, respectively, while a slight decay occurred in the latter, resulting in the following thermodynamic parameters of denaturation: 14.3 kJ/mol activation energy as well as 5.6–9.7 kJ/mol standard Gibbs free energy, 15.6 kJ/mol standard enthalpy and 18.3–29.0 J/(K·mol) standard entropy variations. Conversely, tannase immobilized on nanoparticles displayed a typical linear decay trend with 43.8 kJ/mol activation energy, 99.2–103.1 kJ/mol Gibbs free energy, 41.1–41.3 kJ/mol enthalpy and −191.6/−191.0 J/(K·mol) entropy of denaturation. A 90-day shelf-life investigation revealed that tannase immobilized on nanoparticles was approximately twice more stable than the one immobilized in calcium alginate beads, which suggests its use and recycling in food industry clarification operations. To the best of our knowledge, this is the first comparative study on kinetic and thermodynamic parameters of a tannase produced by *A. ficuum* in its free and immobilized forms.

Keywords: tannase; *Aspergillus*; immobilization; calcium alginate beads; magnetic nanoparticles; kinetics; thermodynamics

Citation: de Carvalho-Silva, J.; da Silva, M.F.; de Lima, J.S.; Porto, T.S.; de Carvalho, L.B., Jr.; Converti, A. Thermodynamic and Kinetic Investigation on *Aspergillus ficuum* Tannase Immobilized in Calcium Alginate Beads and Magnetic Nanoparticles. *Catalysts* **2023**, *13*, 1304. https://doi.org/10.3390/catal13091304

Academic Editors: Chia-Hung Kuo, Chwen-Jen Shieh and Hui-Min David Wang

Received: 24 August 2023
Revised: 14 September 2023
Accepted: 16 September 2023
Published: 18 September 2023

1. Introduction

The immobilization of enzymes, when combined with the fundamental principles of thermodynamics and kinetics, has proven to be a highly useful tool for the successful application of biocatalysis in industrial processes [1,2]. If, on the one hand, immobilization can enhance the stability and reusability of a biocatalyst, on the other hand, knowledge of kinetic and thermodynamic parameters—such as decimal reduction time, half-life,

activation energy, Gibbs free energy, enthalpy and entropy—is essential to predict the reaction mechanism and behavior of any process using immobilized enzymes as well as biocatalyst thermostability at a given operating temperature [1–3]. These aspects taken together are key issues that must be considered to make the application of enzyme-based industrial processes even more economic [1,4].

Tannase (or tannin acyl hydrolase, E.C. 3.1.1.20) is a biotechnologically important enzyme that catalyzes the hydrolysis of ester and depside bonds present in tannins, such as tannic acid among others, and releases gallic acid and glucose [5]. For this reason, many industrial processes require tannase to improve their efficiency [6–8]. Such an enzyme can be extracted from vegetable and animal sources. However, for being an extracellular enzyme, microorganisms are its main producers for industrial applications [6]. Among them, fungi (e.g., *Aspergillus* species) [7], bacteria [8] and yeasts [9] are generally used for large scale production of tannases, since their enzymes are very stable in wide pH and temperature ranges [7,9,10].

Being versatile enzymes, tannases have a lot of different applications in a number of industrial sectors, such as food, beverage, animal feed, chemical and pharmaceutical industries, as well as in wastewater treatment and other bioprocesses [6,7]. In particular, thanks to their capability of increasing tannin solubility, tannases are broadly used to improve the clarification of beer, juices and wine, thus reducing turbidity, improving color appearance, and softening the costumer's undesired astringent taste of tannins [8,11].

Despite its undisputed potential, the drawbacks connected with the use of free enzymes like tannases in industrial applications (e.g., insufficient stability and inability to recover/recycle the biocatalyst) make the process expensive [7,12]. Enzyme immobilization is one of the strategies developed to overcome these limitations [7,12,13]. After immobilization, some features of the enzymes can change, being able to improve their catalytic capacity and thermal stability, vary the pH range where they can be used, as well as facilitate their separation/recovery by simple physical operations [12,14–16].

According to the required application, research efforts have focused on the development of more effective enzyme immobilization techniques with better catalytic features, seeking suitable/attractive carrier materials to be used as biocompatible support matrices to immobilize biomolecules. However, according to Silva et al. [14], upon immobilization the enzyme activity may be altered by some factors such as crosslink agents, binding mode, microenvironment, diffusion, protein aggregation, molecular polarization, partition, conformational changes, induction and structural flexibility.

Larosa et al. [17] have reported that, among the various available immobilization methods, entrapment in calcium alginate beads is an effective method to immobilize tannase and to preserve its catalytic activity because it does not involve chemical modification, thereby ensuring easiness of use, mild conditions and low cost as its main advantages. Recently, Intisar et al. [18] have reported that alginate biopolymer, an anionic polysaccharide derived from brown seaweeds [19], has gained noteworthy consideration from researchers and industrialists as a suitable material for developing entrapped enzyme preparations with enhanced activities because of its versatile characteristics, such as no toxicity, relatively high availability, low cost, simple preparation, good biocompatibility and reusability.

On the other hand, according to Cabrera et al. [20], diatomaceous earth, a lightweight mineral clay composed especially of amorphous hydrated silica, has gained attention thanks to its favorable properties, such as low cost, ready availability, high cation exchange capacity, chemical inertness, porous structure, large surface area, and low thermal conductivity. In previous studies, *Aspergillus ficuum* tannase was immobilized by two different techniques, namely entrapment in calcium alginate beads [19] and covalent immobilization onto magnetic nanoparticles composed of diatomaceous earth coated with polyaniline [21]. The results of these works suggest that immobilized tannase systems are promising in food applications to improve tea quality and to remove tannins from aromatic beverages.

Nowadays, enzyme immobilization and kinetic/thermodynamic studies have attracted much interest [1,22–24]. Indeed, an overview of the literature published over the

last two years up to the beginning of August 2023 has revealed that there has been an increase in the contributions related to "enzyme immobilization and thermodynamic and kinetic", with no less than 815 research articles (based on the Science Direct search engine: http://www.sciencedirect.com, accessed on 10 August 2023). However, there are a few investigations on the kinetic and thermodynamic parameters of immobilized or free tannases, especially those of the comparative type like this.

Based on this background, the present work aimed to determine the kinetic and thermodynamic parameters of activity and thermal stability of *A. ficuum* tannase immobilized either in calcium alginate beads or on magnetic nanoparticles. For this purpose, the performance of both preparations was compared for the first time to that of the free enzyme, providing valuable information for a better understanding of reaction mechanism and performance prediction in possible enzyme-based industrial applications.

2. Results and Discussion

The *Aspergillus ficuum* tannase was previously immobilized on two supports with different techniques, namely entrapment in calcium alginate beads [19] and covalent immobilization on magnetic nanoparticles composed of polyaniline-coated diatomaceous earth (mDE-PANI-tannase) [21]. In this work, both immobilized-enzyme preparations were subjected to kinetic and thermodynamic modeling to determine the parameters involved in both catalysis and protein thermal denaturation, whose related equations and definitions have been mostly reported for two different enzyme preparations [25,26] and partially summarized in Section 3.3. In addition, a comparative study of such parameters with those of the free enzyme was also performed.

2.1. Thermodynamic Parameters of Tannase-Catalyzed Reaction

Figure 1A illustrates the straight lines obtained by plotting, according to Arrhenius, the experimental results of tannin hydrolysis using free tannase, tannase immobilized in calcium alginate beads and mDE-Pani-tannase. In particular, the straight lines on the right refer to the increase in activity, described by the Arrhenius equation, resulting from a temperature rise from 20 to 40 °C for both immobilized enzyme preparations and from 20 to 30 °C for the free enzyme. This 10 °C difference in the optimal temperature of catalysis (T_{opt}) can be ascribed to conformational changes that the enzyme underwent due to immobilization in different supports [21]. Free tannase exhibited the highest activation energy of reaction (E) (51 kJ/mol, R^2 = 0.98) followed by tannase immobilized in calcium alginate beads (31.3 kJ/mol, R^2 = 0.96) and by mDE-PANI-tannase (15.1 kJ/mol, R^2 = 0.99). The lowest value of E observed for the enzyme immobilized on magnetic nanoparticles could have been due to the covalent nature of bonds involved in such a type of immobilization, which may have allowed the enzyme to be present only on the support surface and therefore more available for contact with the substrate [14]. As reported by Fernandes et al. [27], lower activation energies are desirable for commercial enzymes, as they imply lower expenses during the process.

Unlike what occurred for E, the standard enthalpy variation of the enzyme unfolding equilibrium (ΔH°_{u}) [25,26], which was estimated from the slopes of straight lines obtained at temperatures higher than T_{opt} (on the left in Figure 1A), showed an opposite behavior, with the highest value being observed for tannase immobilized in calcium alginate beads (29.6 kJ/mol, R^2 = 0.97), followed by mDE-PANI-tannase (17.6 kJ/mol, R^2 = 0.90) and free tannase (17.6 kJ/mol, R^2 = 0.99). In this case, the higher this value, the greater the stability of the biocatalyst at high temperatures [4]. This outcome corroborates with what was expected from the technique used to immobilize tannase. The entrapment technique confined the enzyme within the matrix, which gave it greater protection against sudden variations or prolonged exposure to a given temperature. As explained better by Boudrant et al. [28], a proper immobilization protocol is important to achieve higher performance of the biocatalist and mainly to enhance its stability.

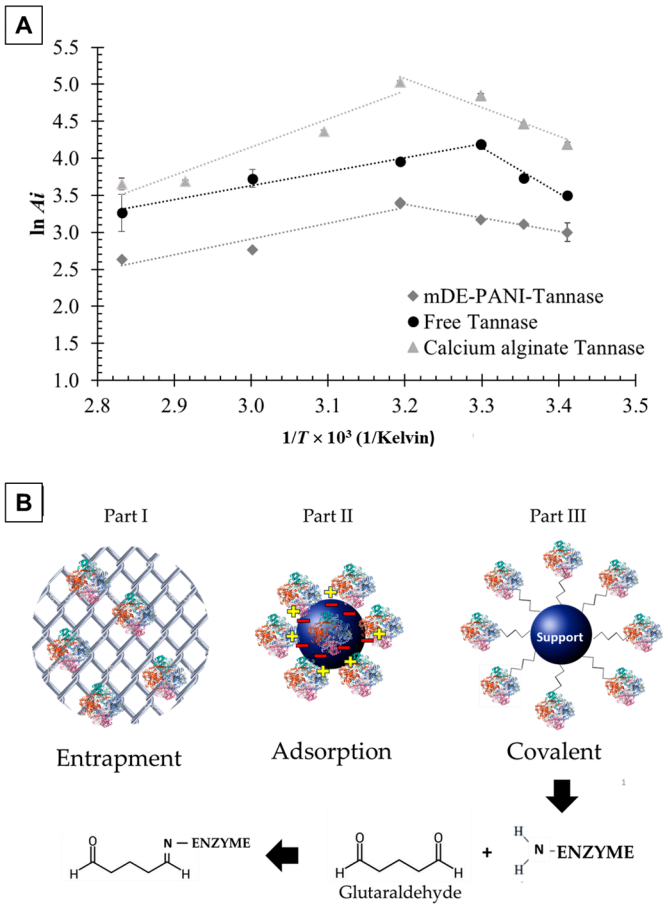

Figure 1. (**A**) Arrhenius-type plots for determination of the activation energy of the reaction catalyzed by free tannase, tannase entrapped in calcium alginate beads and tannase covalently immobilized on magnetic nanoparticles (mDE-PANI-tannase). (**B**) Schematic representations of the main immobilization techniques.

The entrapment technique imprisons the enzyme molecules inside the support (Figure 1B, part I), and the pore size influences directly the enzyme activity. Differently from adsorption (Figure 1B, part II) and covalent immobilization, it does not use chemical bonds or electrostatic forces, and the enzyme is physically trapped in the matrix. On other hand, covalent immobilization (Figure 1B, part III) resorts to chemical bonds. However, the enzyme structure cannot make a bond with polymer supports like alginate and polyaniline, for which a powerful crosslinking agent such as glutaraldehyde is needed. Glutaraldehyde, a bifunctional compound with an aldehyde group in each extremity, is able to make a chemical bond with amino groups from the side chains (Figure 1B, part III); so, the enzyme is immobilized on the support surface. Both techniques have their advantages depending mainly on the application [14].

It is noteworthy that the parameter ΔH°_{u} refers to the enthalpic energy related to enzyme unfolding, which interferes with the formation of enzyme-substrate complex. As previously described by Abellanas-Perez et al. [29], the enzyme has a specific affinity for a particular substrate, which depends on its tridimensional structure; so, any change in structure leads to a loss in biological activity. As explained by Da Silva et al. [4], the tridimensional structures of enzymes are supported by non-covalent bonds such as hydrogen bonds, Van der Waals forces, dipole-dipole interactions, ion exchange, etc., which are easily broken by motion due to a temperature increase. At low temperatures there is little vibration, and enzyme molecules are present in rigid forms. At higher temperatures, due to some breaks of these bonds, enzyme molecules undergo structural modifications and acquire more malleable conformations, which allows the substrate to more easily fit

in the active site and, as a consequence, the affinity to increase. However, when too many bonds are broken simultaneously, the enzyme cannot form its complex with the substrate, and thus a decline in the reaction rate is observed [30].

2.2. Thermodynamics of Tannase Thermal Inactivation

As explained earlier, thermodynamics of thermal inactivation of the enzyme is related to energy involved in the loss of protein structure. This occurs when the enzyme is subjected to prolonged exposure to a given temperature.

2.2.1. Free Tannase Thermal Inactivation

Figure 2A shows the straight lines obtained by plotting the natural logarithm of the free enzyme residual activity (Ψ) as a function of time at different temperatures in order to determine the related constants of thermal inactivation (denaturation) (k_d). These k_d values were later used to estimate the activation energy of free enzyme thermal inactivation (E_d = 53.5 kJ/mol) through the Arrhenius equation (Figure 2B). The straight lines showed high determination coefficients (R^2), and the values of kinetic and thermodynamic parameters of free tannase denaturation are listed in Table 1.

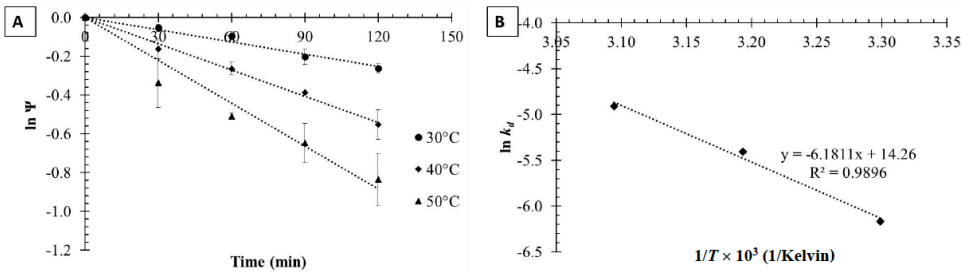

Figure 2. Semi-log plots of residual activity (Ψ) of free tannase vs. time at different temperatures (**A**) and Arrhenius-type semi-log plot of the first-order denaturation constant (k_d) vs. reciprocal temperature ($1/T$) used to estimate the activation energy of free tannase thermal inactivation (**B**).

Table 1. Kinetic and thermodynamic parameters of free tannase denaturation.

Temperature (°C)	k_d [1] (min^{-1})	R^2	ΔH_d [2] (kJ/mol)	ΔG_d [3] (kJ/mol)	ΔS_d [4] (J/(K·mol))	$t_{1/2}$ [5] (min)	*D*-Value [6] (min)
30	0.0021	0.98	50.99	100.15	−162.15	330.07	1096.67
40	0.0045	0.99	50.91	101.55	−161.72	154.03	511.78
50	0.0074	0.98	50.82	103.54	−163.13	93.67	311.22

[1] k_d = first-order denaturation constant. [2] ΔH_d = activation enthalpy of denaturation. [3] ΔG_d = activation Gibbs free energy of denaturation. [4] ΔS_d = activation entropy of denaturation. [5] $t_{1/2}$ = half-life. [6] *D*-value = decimal reduction time.

The activation Gibbs free energy of enzyme denaturation (ΔG_d), which reflects the amount of remaining energy in the protein structure after exposure to a certain temperature [31], increased from 100.15 kJ/mol at 30 °C to 103.54 kJ/mol at 50 °C, thereby highlighting a certain thermal stability. This result suggests that, within the tested temperature range and exposure time (120 min), free tannase denaturation was likely to be reversible, as better explained in Section 3.3. Such an assumption is corroborated by the negative values of activation entropy of free tannase denaturation listed in Table 1 (ΔS_d). In fact, according to Wahba et al. [23], negative entropy values suggest greater enzyme stability and that the irreversible denaturation process is a further step forward involving higher temperatures and longer times.

Consistently, the enthalpy of denaturation (ΔH_d), which reflects the amount of broken non-covalent bonds, showed only a slight variation. In fact, considering that the energy to break a non-covalent bond can be estimated at about 5.4 kJ/mol [30], in the temperature range under investigation only 9 non-covalent bonds were likely to be broken in

free tannase, a number that does not seem to have been sufficient for the denaturation process to become irreversible. In this respect, it is important to notice that enzymes with thermostability characteristics in their free form are more suitable to be immobilized in supports, as they can be recovered for later applications.

Other kinetic parameters evaluated for free tannase were the half-life ($t_{1/2}$) and the decimal reduction time (*D*-value), which characterize the thermal inactivation behavior at each temperature to which an enzyme is exposed [24]. Both decreased by increasing temperature, showing the temperature influence in reducing the overall activity due to thermal inactivation. The thermal resistance constant (*Z*-value), a parameter of sensitivity to temperature variation, was then estimated from the slope of thermal– death–time plot of log*D*-value versus temperature. It revealed that an increase of about 19 °C is required for *D*-value to be reduced by one log cycle, i.e., by 90% [14].

2.2.2. Thermal Inactivation of Tannase Immobilized on Magnetic Nanoparticles

The kinetic and thermodynamic parameters of thermal inactivation of mDE-PANI-tannase were close to those found for the free enzyme. As can be seen in Figure 3, the semi-log plots used to determine the values of k_d (Figure 3A) and E_d (Figure 3B) showed high R^2 values (Table 2), demonstrating that mDE-PANI-tannase behavior can be described by the equations outlined in Section 3.3. However, this tannase immobilization technique reduced the value of E_d to 43.9 kJ/mol, i.e., by approximately 10 kJ/mol compared to the free enzyme. Considering that the higher this parameter, the greater the stability of a biocatalyst, such a reduction suggests that the enzyme was slightly more sensitive to temperature variations [14].

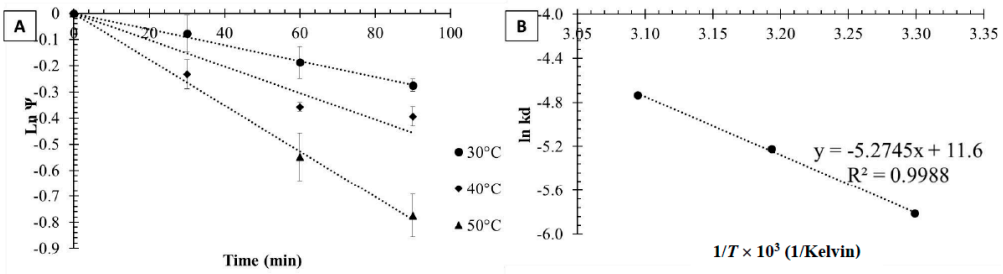

Figure 3. Semi-log plots of residual activity (Ψ) of mDE-PANI-tannase (starting hydrolysis specific activity of 342 U/mg) vs. time at different temperatures (**A**) and Arrhenius-type semi-log plot of the first-order denaturation constant (k_d) vs. reciprocal temperature ($1/T$) used to estimate the activation energy of mDE-PANI-tannase thermal inactivation (E_d) (**B**).

Table 2. Kinetic and thermodynamic parameters of mDE-PANI-tannase denaturation.

Temperature (°C)	k_d [1] (min^{-1})	R^2	ΔH_d [2] (kJ/mol)	ΔG_d [3] (kJ/mol)	ΔS_d [4] (J/(K·mol))	$t_{1/2}$ [5] (min)	*D*-Value [6] (min)
30	0.0030	0.99	41.33	99.25	−191.04	231.05	767.67
40	0.0054	0.96	41.25	101.08	−191.05	128.36	426.48
50	0.0088	0.99	41.17	103.08	−191.58	78.77	261.70

[1] k_d = first-order denaturation constant. [2] ΔH_d = activation enthalpy of denaturation. [3] ΔG_d = activation Gibbs free energy of denaturation. [4] ΔS_d = activation entropy of denaturation. [5] $t_{1/2}$ = half-life. [6] *D*-value = decimal reduction time.

This behavior is corroborated by the decrease of *Z*-value from 19 to 16 °C. The values of the other kinetic denaturation parameters, namely, *D*-value and $t_{1/2}$ (Table 2), were also smaller than those of free tannase (Table 1), confirming the lower thermostability of this enzyme preparation.

ΔG_d increased from 99.25 to 103.08 kJ/mol with increasing temperature from 30 to 50 °C (Table 2), suggesting that tannase maintained its reversible profile of thermal denaturation after immobilization on magnetic nanoparticles. This occurrence is consistent with the results

of de Lima et al. [21], who reported that tannase immobilized on magnetic diatomaceous earth nanoparticles coated with polyaniline could be reused up to 10 times losing only 34% of its initial activity. ΔS_d also had negative values (−191.58/−191.04 J/(K·mol)), which are characteristic of reversible inactivation. Finally, ΔH_d (41.17–41.33 kJ/mol) was reduced by almost 10 kJ/mol compared to the free enzyme, which corresponds to the breakdown of approximately eight non-covalent bonds.

2.2.3. Thermal Inactivation of Tannase Immobilized in Calcium Alginate Beads

Unlike what was expected from a typical thermal stability study, *A. ficuum* tannase entrapped in calcium alginate beads exhibited an unusual behavior throughout the whole tested temperature range (20–70 °C). While the free form of tannase and the mDE-PANI-tannase showed the characteristic decay profile of protein denaturation (Figures 2A and 3A), the activity of tannase entrapped in alginate beads, after an initial increase until a maximum value after about 30 min, progressively decreased still keeping above its starting value (Figure 4). This behavior is not commonly observed. Only Rodríguez-Lopez et al. [32] reported the same behavior for mushroom polyphenol oxidase upon inactivation using an 80 °C hot water bath and 22.6 W/cm^3 microwave power irradiation. However, there is no mathematical model available in the literature on other biocatalysts that acted in the same or similar way.

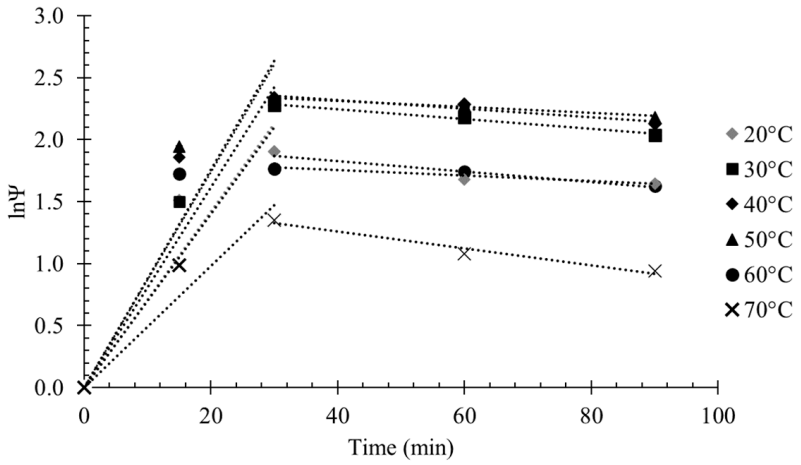

Figure 4. Semi-log plots of residual activity (Ψ) of tannase entrapped in calcium alginate beads (starting hydrolysis activity of 127.5 U/mL) vs. time at different temperatures.

Therefore, a new mathematical approach to the kinetic and thermodynamic parameters of the biocatalyst entrapped in calcium alginate beads was proposed in the present study. Since the calcium alginate beads were porous polymeric spheres where tannase had been entrapped, they may have suffered leaching due to exposition to temperatures higher than the optimum one, which may have partially degraded their polymeric structure and increased pore size (Figure 5, part II). Obviously, a similar mechanism can be proposed for the action of other external agents such as suboptimal pH, chemical agents and so on. Therefore, the contact between enzyme and outer environment, i.e., the solvent in the case of residual activity tests performed in this study at temperatures higher than that optimal one or reaction medium in industrial applications, became progressively more effective along the starting 30 minutes. However, when the enzyme was exposed for a longer period, its structure began to be denatured, and there was a decrease in its activity (Figure 5, Part III). Nonetheless, the residual activity still remained above the initial one. Calcium alginate probably conferred extra protection to tannase, so that an activity lower than the initial one would have required exposition longer than 100 min.

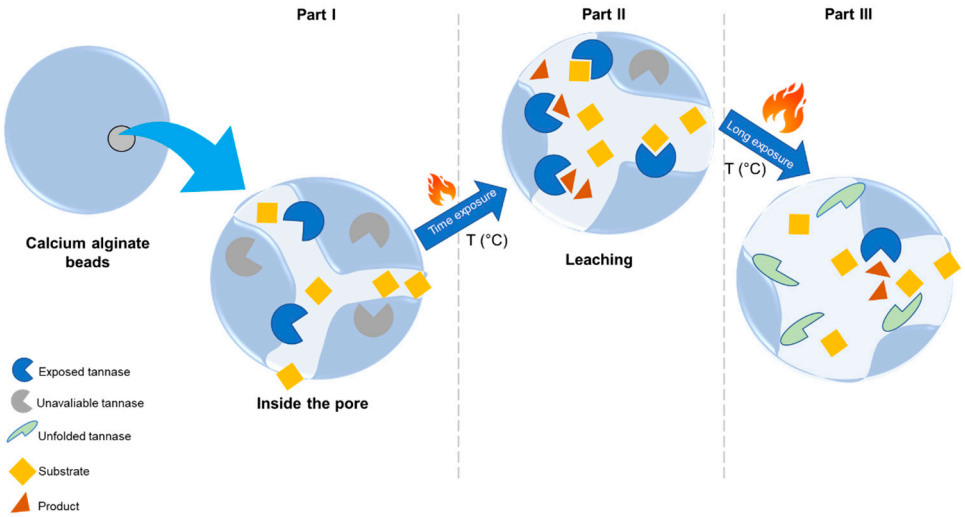

Figure 5. Mechanism proposed in this study for the degradation of calcium alginate beads exposed to temperatures higher than the optimum one.

As mathematically described by Equation (5) onwards in Section 3.3, the kinetic constant of the resultant of these two phenomena is the sum of both positive (k_L) and negative (k_d) contributions in terms of residual activity. The values of these constants are gathered in Table 3 along with the respective determination coefficients.

Table 3. Kinetic constants describing the activity increase due to matrix leaching (k_L) and activity decrease due to subsequent denaturation (k_d) of tannase entrapped in calcium alginate beads.

Temperature (°C)	k_L (min^{-1})	R^2	k_d (min^{-1})	R^2
20	0.079	0.96	0.0043	0.85
30	0.0808	0.99	0.0040	0.99
40	0.087	0.96	0.0035	0.93
50	0.0879	0.95	0.0024	0.95
60	0.070	0.91	0.0023	0.87
70	0.0491	0.97	0.0068	0.96

It is possible to observe in Figure 4 that the straight lines describing the variations of $\ln\Psi$ over time did not obey the traditional one-step decreasing profile as the temperature was raised from 20 to 70 °C. Since these constants are related to the activation energies involved in the two proposed phenomena, it is possible to identify in Figure 6A two different regions, the former between 20 and 50 °C (straight line on the right) and the latter between 50 and 70 °C (straight line on the left). Thus, it was possible to estimate two activation energies linked to the increase in tannase activity resulting from matrix leaching (E_{L1} = 3.1 kJ/mol and E_{L2} = 26.8 kJ/mol, respectively) (Figure 6A) and an activation energy linked to the decrease in activity due to denaturation under prolonged exposure (E_d = 14.3 kJ/mol) (Figure 6B).

As is well known, the Gibbs free energy variation is a parameter that measures the spontaneity of any process, in that, positive values are characteristic of a spontaneous process, negative values of a non-spontaneous process and a null value of a process in thermodynamic equilibrium. As can be observed in Table 4, the standard Gibbs energy variations related to both the activity increase due to leaching of calcium alginate beads (ΔG°_L) and to the activity decrease due to denaturation of the entrapped enzyme after prolonged exposure (ΔG°_d) were negative, demonstrating that the increase in biocatalyst activity was a spontaneous phenomenon characteristic of the support outwear. However, the values of ΔG° that referred to the combination of the two phenomena (ΔG°_{RT}) were positive, suggesting that the increase in activity was a non-spontaneous phenomenon forced by the leaching process.

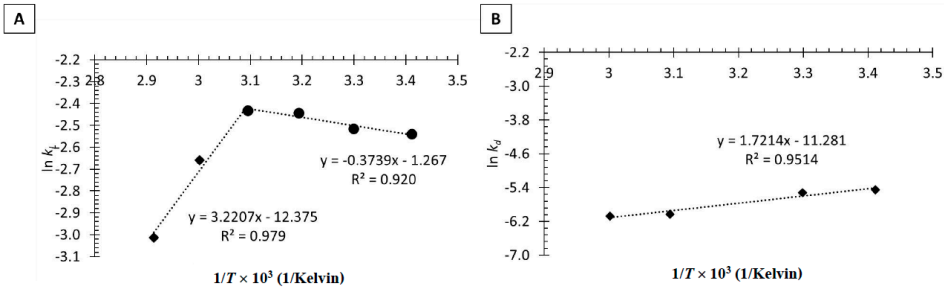

Figure 6. Semi-log plots used to estimate the activation energies linked to the increase in activity resulting from matrix leaching (E_{L1} and E_{L2}) (**A**) and to the decrease in activity due to enzyme denaturation under prolonged exposure (E_d) (**B**). Enzyme system: tannase entrapped in calcium alginate beads.

Table 4. Thermodynamic parameters referred to the activity of tannase entrapped in calcium alginate beads. Parameters referred to the increase in activity resulting from matrix leaching are denoted by the subscript "*L*", those referred to the decrease in activity due to enzyme denaturation under prolonged exposure by the subscript "*d*" and those referred to combination of both phenomena by the subscript "*RT*". Standard variations of Gibbs free energy (ΔG°), enthalpy (ΔH°) and entropy (ΔS°).

Temperature (°C)	ΔG°_L (kJ/mol)	ΔG°_d (kJ/mol)	ΔG°_{RT} (kJ/mol)	ΔH°_L [1] (kJ/mol)	ΔH°_d (kJ/mol)	ΔH°_{RT} (kJ/mol)	ΔS°_L (J/(K·mol))	ΔS°_d (J/(K·mol))	ΔS°_{RT} (J/(K·mol))
20	−87.9	−95.0	7.1	29.9	14.3	15.6	401.9	372.9	29.0
30	−90.9	−98.5	7.6	29.9	14.3	15.6	398.6	372.2	26.4
40	−93.8	−102.2	8.4	29.9	14.3	15.6	395.1	372.1	23.0
50	−96.9	−106.6	9.7	29.9	14.3	15.6	392.3	374.1	18.2
60	−100.6	−110.1	9.5	29.9	14.3	15.6	391.7	373.3	18.4
70	−104.7	−110.4	5.6	29.9	14.3	15.6	392.3	363.3	29.0

[1] ΔH°_L was calculated as the sum (E_L) of both activation energies linked to the activity increase resulting from matrix leaching (E_{L1}) and activity decrease due to denaturation after prolonged exposure (E_{L2}) (Figure 6A and Equation (21)).

Standard enthalpy variations related to increased activity due to support leaching (ΔH°_L) and decreased activity due to denaturation after prolonged exposure (ΔH°_d) did not vary with rising temperature, being 29.9 and 14.3 kJ/mol, respectively, while the one that referred to the combination of the two phenomena (ΔH°_{RT}) was 15.6 kJ/mol in the entire temperature range studied. This value corresponds approximately to the breaking of only three non-covalent bonds after 90 min of biocatalyst exposure. Finally, the fact that the related entropy variations were positive and very small ($18.2 \leq \Delta S^\circ_{RT} \leq 29.0$ J/(K·mol)) confirms that, despite representing an irreversible denaturation process, such thermal inactivation was poorly significant and that the biocatalyst had excellent thermostability.

2.2.4. Inactivation of Immobilized Enzyme under Storage Conditions

Tannase immobilized either on magnetic nanoparticles or in calcium alginate beads was finally subjected to a shelf-life study to determine the kinetic parameters often used to characterize the stability of enzyme preparations to be used in industrial applications, i.e., the half-life ($t_{1/2}$) and the decimal reaction time (*D*-value).

During experiments for 90 days at 4 °C (Figure 7) mDE-PANI-tannase showed significantly greater stability than tannase entrapped in calcium alginate beads. Indeed, $t_{1/2}$ (217 days) and *D*-value (720 days) of the former preparation were almost twice those of the latter ($t_{1/2}$ = 116 days; *D*-value = 384 days).

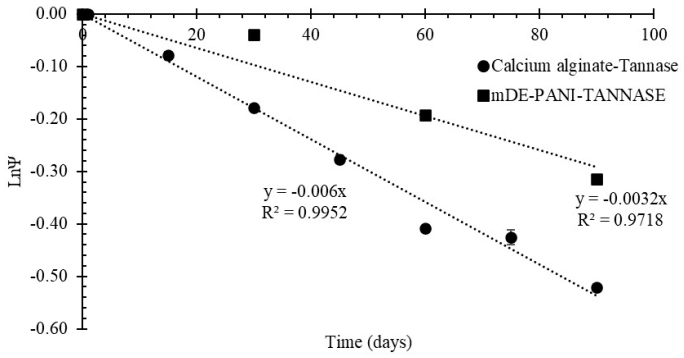

Figure 7. Semi-log plots of the residual activity coefficient (Ψ) vs. time during shelf-life experiments at 4 °C of *A. ficuum* tannase immobilized in calcium alginate beads and on magnetic nanoparticles (mDE-PANI-tannase).

3. Materials and Methods

Commercial tannase (300 U/g) from *Aspergillus ficuum* used in this study was purchased from Sangherb Bio-Tech (Xi'an, China). It was immobilized either in calcium alginate beads or on magnetic nanoparticles.

3.1. Tannase Immobilization

3.1.1. Immobilization in Calcium Alginate Beads

Tannase was entrapped in calcium alginate beads as described by de Lima et al. [19]. Briefly, 10 mL of *A. ficuum* tannase solution (6 mg/mL, corresponding to enzyme activity of 127.5 U/mL) in 0.2 M acetate buffer, pH 5.0, were mixed with 30 mL of 3.0% (*w*/*v*) sodium alginate solution and dropped in 60 mL of 2.0% (*w*/*v*) $CaCl_2$ solution at 4 °C under stirring for beads formation. The resulting tannase-loaded beads, with approximately 0.4 mm mean diameter, were left to cure in the same $CaCl_2$ solution for 4.0 h, collected, washed twice with distilled water, suspended in the above working buffer and finally stored at 4 °C for further use.

3.1.2. Immobilization on mDE-PANI Nanoparticles

Diatomaceous earth (DE) particles were magnetized (mDE) according to Cabrera et al. [20]. A black precipitate was collected and coated with polyaniline (PANI) as follows. The precipitate was submitted to treatment with 0.1 M $KMnO_4$ solution at 25 °C for 60 min, and nanoparticles were washed with distilled water and immersed into 0.25 M aniline solution prepared in 2.0 M HCl at 4 °C for 30 min. Then, they were washed with distilled water and 1.0 M HCl to remove residual aniline using an external 0.6-T magnetic field (Ciba Corning Medical Diagnostics, Walpole, MA, USA). Finally, mDE-PANI nanoparticles were washed several times, dried at 50 °C and stored at 25 °C for later use.

mDE-PANI nanoparticles were activated with glutaraldehyde (2.5% (*v*/*v*)) by stirring at 25 °C for 2 h and washed several times with distilled water for eliminating unreacted glutaraldehyde. Tannase from *A. ficuum* prepared in 0.2 M sodium acetate buffer (1 mL of 3 mg/mL solution, corresponding to 342 U/mg specific activity), pH 5.0, was incubated with mDE-PANI nanoparticles (0.05 g) at 4 °C under mild stirring for 20 h. Then, tannase immobilized on mDE-PANI nanoparticles (mDE-PANI-tannase) was collected by an external 0.6-T magnetic field, and the supernatants were used for protein determination according to the Bradford method [33] using bovine serum albumin as a standard. The immobilized derivatives were stored in sodium acetate buffer at 4 °C until use.

3.2. Determination of Free and Immobilized Tannase Activity

Tannase activity was measured according to Pinto et al. [34]. Briefly, 0.1 mL of the free enzyme solution in 0.2 M acetate buffer, pH 5.0, or 15 calcium alginate beads with immobilized tannase or 100 μg of tannase immobilized on 0.05 g mDE-PANI were added to

2.0 mL of 0.05% (*w*/*v*) tannic acid solution. After homogenization for 7 min at 30 °C, 100 µL of this reaction mixture were added to 150 µL of ethanolic rhodanine solution (0.667% *w*/*v*) and allowed to react for 5 min. Then, 100 µL of 0.5 M KCl and, after 2.5 min, 2.15 mL of distilled water were added to the mixture. The formation of a complex with maximum absorbance at 520 nm was followed by means of a UV–Vis spectrophotometer, model Lambda 25 (Perkin Elmer, Wellesley, MA, USA). One unit of tannase was defined as the amount of enzyme necessary to obtain 1 µmol of gallic acid per minute under the assay conditions (30 °C for 7 min). Control experiments were also performed using immobilized beads without tannase [19].

3.3. Thermodynamic Modeling

Tannase, either free or immobilized in calcium alginate beads or magnetic nanoparticles, was incubated for 2 h in 0.2 M sodium acetate buffer, pH 5.0, at various temperatures (from 20 to 90 °C), and the residual enzyme activities were determined as described in Section 3.2.

Activation energy of the enzyme-catalyzed reaction (E) and standard enthalpy variation of the enzyme unfolding equilibrium ($\Delta H^{\circ}{}_{u}$) were estimated from semi-log plots of the starting enzyme activity (A_i) versus the reciprocal temperature ($1/T$) in the temperature range of 20–70 °C. In particular, as described elsewhere [25,26], the linearized log form of the Arrenhius equation was used to estimate E in the temperature ranges of 20–40 °C for immobilized enzyme preparations and 20–30 °C for free tannase:

$$A_i = A_o e^{-\frac{E}{RT}} \quad (1)$$

while $\Delta H^{\circ}{}_{u}$ was estimated from the slope of the left straight line of the Arrhenius-type plot of $\ln A_i$ at temperatures higher than the optimal ones (30 and 40 °C, respectively).

Thermal inactivation of most free or covalently immobilized enzymes can be described by the following general deactivation model [35]:

$$N \underset{k\prime_2}{\overset{k\prime_1}{\rightleftarrows}} U \overset{k\prime_3}{\rightarrow} D \quad (2)$$

where N is the native biomolecule in its totally active state, while U and D the biomolecule in its reversibly unfolded and ultimate irreversibly denatured states, while k'_1, k'_2 and k'_3 are the rate constants of enzyme unfolding, folding and denaturation, respectively.

This was the case of both free tannase and tannase immobilized on magnetic nanoparticles, for which the traditional kinetic and thermodynamic approach proposed for other enzyme systems was successful [25,26].

However, after immobilization some enzymes may become more thermostable due to variations in their tertiary structure induced by crosslinking agents or the matrix itself. Since the entrapment of enzymes in calcium alginate beads implies their immobilization within the matrix during the gelation process (Figure 5, part I), the access of substrate takes place through the polymer pores. Organic polymers like this may be subject to degradation when exposed to chemical, physical or microbiological agents. In this case, their pores may increase in size and number, leaving the immobilized enzyme, i.e., tannase in this study, more exposed to the reaction medium and allowing the substrate to enter the pores more easily (Figure 5, part II). Equation (2) can then be rewritten in order to take into account such an increase in enzyme activity due to exposure of the polymeric matrix to these agents:

$$I \overset{k_0}{\rightarrow} A \underset{k_2}{\overset{k_1}{\rightleftarrows}} U \overset{k_3}{\rightarrow} D \quad (3)$$

where I and A are the immobilized-enzyme preparations at the beginning and after exposure, k_o is the rate constant of this phenomenon, while k_1, k_2 and k_3 are the new unfolding, folding and denaturation constants.

Assuming that polymer degradation is an irreversible and first-order process, enzyme activity tends to increase over time:

$$\frac{dA}{dt} = kA \tag{4}$$

where k is the overall kinetic constant and A the enzyme activity.

Because enzymes are molecules with biological activity, they progressively lose their activity due to the denaturation process. In fact, when exposed for long time to agents such as high temperature in the present case, non-covalent bonds can be broken, and their three-dimensional structure becomes predominantly unfolded (Figure 5, part III). Normally, as is the case of free tannase and tannase immobilized on magnetic nanoparticles, this decay shows a linear trend and can be treated as an irreversible first-order reaction. On the other hand, in the case of tannase entrapped in calcium alginate beads, k is influenced by these opposite contributions, i.e., the activity increase resulting from polymer degradation, described by the degradation constant (k_L), and the activity reduction due to enzyme denaturation described by the denaturation constant (k_d):

$$k = k_L - k_d \tag{5}$$

The contribution of the former phenomenon is more pronounced than that of the latter when $k > 0$, and vice versa when $k < 0$. To better understand the meaning of this constant, it is important to remember that the enzyme is in a thermodynamic folding/unfolding equilibrium, which is governed by k_1 and k_2, while the formation of final product is governed by k_3. The overall kinetic constant can then be written as follows [36]:

$$k = \frac{k_1\, k_3}{k_2 + k_3} \tag{6}$$

By equaling Equations (5) and (6), we obtain the Equation:

$$k_L - k_d = \frac{k_1\, k_3}{k_2 + k_3} \tag{7}$$

that simplifies to Equation (8) when $k_3 \ll k_2$:

$$k_L - k_d = k_3\, K_{eq} \tag{8}$$

where K_{eq} is the constant of the folding/unfolding equilibrium.

Considering that $k_3 = \frac{k_B T}{h}$ [37], one can write:

$$K_{eq} = \frac{k_L h}{k_B T} - \frac{k_d h}{k_B T} \tag{9}$$

where T is the absolute temperature, h the Planck's constant, and k_B the Boltzmann's constant.

To describe the thermal inactivation kinetics, Ortega et al. [38] proposed a multi-fraction inactivation model, which supposes the existence of multiple enzyme fractions, each of which can be independently analyzed with first-order kinetics. Considering the well-known relationship between the standard variation of Gibbs free energy (ΔG°) and K_{eq}:

$$\Delta G^o = -RT \ln K_{eq} \tag{10}$$

and applying the approach of Ortega et al. [38] to the above two contributions governed by k_L and k_d, we can calculate this parameter for the tannase system under investigation ($\Delta G^\circ{}_{TR}$) as:

$$\Delta G^o{}_{TR} = -\left(RT \ln \frac{k_L h}{k_B T} - RT \ln \frac{k_d h}{k_B T} \right) \tag{11}$$

Considering that:

$$\Delta G^o = \Delta H^o - T\Delta S^o \tag{12}$$

under the equilibrium conditions described above, $\Delta G^\circ{}_{TR}$ can also be described by the equation:

$$\Delta G^o{}_{TR} = (\Delta H^o{}_L - T\Delta S^o{}_L) - (\Delta H^o{}_d - T\Delta S^o{}_d) \tag{13}$$

By equaling the right members of Equations (11) and (13), we obtain:

$$RT \ln\left(\frac{k_d}{k_L}\right) = \Delta H^o{}_L - T\Delta S^o{}_L - \Delta H^o{}_d + T\Delta S^o{}_d \tag{14}$$

$$RT \ln\left(\frac{k_d}{k_L}\right) = \Delta H^o{}_L - \Delta H^o{}_d + T(\Delta S^o{}_d - \Delta S^o{}_L) \tag{15}$$

$$\ln\left(\frac{k_d}{k_L}\right) = \frac{\Delta H^o{}_L}{RT} - \frac{\Delta H^o{}_d}{RT} + \frac{(\Delta S^o{}_d - \Delta S^o{}_L)}{R} \tag{16}$$

By differentiating Equation (16) with respect to T, we can write:

$$\frac{d\left(\ln \frac{k_d}{k_L}\right)}{dT} = -\frac{\Delta H^o{}_L}{RT^2} + \frac{\Delta H^o{}_d}{RT^2} \tag{17}$$

Applying the Arrhenius equation to the two above-mentioned contributions governed by k_L and k_d, we can write the equation:

$$\frac{k_d}{k_L} = \frac{A_o \, e^{-E_L/RT}}{B_o \, e^{-E_d/RT}} \tag{18}$$

where E_L and E_d are their respective activation energies, while A_o and B_o are the corresponding pre-exponential factors.

The linearized version of this equation:

$$\ln \frac{k_d}{k_L} = -\frac{(-E_L + E_d)}{RT} + \ln \frac{A_o}{B_o} \tag{19}$$

can be differentiated with respect to T to omit the constant term, thus leading to the equation:

$$\frac{d\left(\ln \frac{k_d}{k_L}\right)}{dT} = \frac{(-E_L + E_d)}{RT^2} \tag{20}$$

Equaling the right terms of Equations (17) and (20), the enthalpy of the reaction catalyzed by tannase entrapped in calcium alginate beads can be calculated as the difference of E_d and E_L:

$$\Delta H^o{}_{RT} = \Delta H^\circ{}_d - \Delta H^\circ{}_L = E_d - E_L \tag{21}$$

Considering Equation (12), one can calculate the entropy of tannase-catalyzed reaction for this enzyme preparation by the equation:

$$\Delta S^\circ{}_{RT} = \frac{\Delta H^\circ{}_{RT} - \Delta G^\circ{}_{RT}}{T} \tag{22}$$

3.4. Shelf Life Stability of the Immobilized Enzyme Preparations

Storage stability of both free and immobilized tannase, with starting activity of about 170 U/mL, was checked by determining the residual activity after long-time storage (90 days) at 4 °C. Free tannase was stored as solution in 0.2 M acetate buffer, pH 5.0, while the immobilized one was stored in wet form. Enzyme activity was determined at regular time intervals (15 days). The kinetic shelf-life parameters of tannase immobilized

either in mDE-PANI or in calcium alginate beads were evaluated for 90 days to 4 °C. The enzyme activity was performed every 15 days using tannic acid as a substrate as described in Section 3.2. k_d, $t_{1/2}$ and *D*-value were determined as described by Silva et al. [14].

4. Conclusions

The *Aspergillus ficuum* tannase, which was immobilized either by entrapment in alginate calcium beads or covalently on magnetic nanoparticles, showed good stability when subjected to different temperatures and exposed to the solvent for a long period. The thermodynamic analysis of the reaction revealed that tannase immobilized on nanoparticles had the lowest activation energy and, therefore, would be the most appropriate enzyme preparation to conduct low-cost industrial tannin degradation treatments. However, thermodynamics and kinetics of biocatalyst denaturation showed that, although the enzyme either in its free or immobilized form is subject to a reversible denaturation mechanism, calcium alginate immobilization ensured greater stability for longer. Using this entrapment technique, tannase hydrolytic activity was increased due to leaching of support accompanied by pore enlargement, which, in addition to allowing greater biocatalyst contact with the substrate, provided greater protection against thermal inactivation after 90 min of incubation. Finally, shelf-life tests performed on immobilized biocatalysts at 4 °C for 90 days revealed that the enzyme immobilized on magnetic nanoparticles kept its activity for almost twice the time as the enzyme entrapped in calcium alginate beads. Such findings suggest that this tannase in both immobilized forms, which showed great potential for tannin degradation and thermal stability, could be profitably exploited for applications in the food industry.

Author Contributions: Conceptualization, A.C., J.d.C.-S., M.F.d.S. and T.S.P.; methodology, J.d.C.-S., A.C., M.F.d.S. and J.S.d.L.; software, J.d.C.-S., A.C., M.F.d.S. and T.S.P.; validation, A.C., J.d.C.-S., M.F.d.S. and T.S.P.; formal analysis, J.d.C.-S., J.S.d.L. and M.F.d.S.; investigation, J.d.C.-S., A.C., J.S.d.L. and M.F.d.S.; resources, L.B.d.C.J., A.C. and T.S.P.; data curation, J.d.C.-S., A.C. and M.F.d.S.; writing—original draft preparation, J.d.C.-S. and M.F.d.S.; writing—review and editing, J.d.C.-S., M.F.d.S., T.S.P. and A.C.; visualization, J.d.C.-S., M.F.d.S., A.C. and T.S.P.; supervision, A.C., L.B.d.C.J. and T.S.P.; project administration, A.C., L.B.d.C.J. and T.S.P.; funding acquisition, L.B.d.C.J., A.C. and T.S.P. All authors have read and agreed to the published version of the manuscript.

Funding: This study was funded in part by the CAPES (Coordenação de Aperfeiçoamento de Pessoal de Nível Superior–Brazil, grant number 88881.131854/2016-01).

Data Availability Statement: Not applicable.

Acknowledgments: J.D.C.S. would like to thank FACEPE (Foundation for Science and Technology support of the Pernambuco State, Recife, Brazil) for complementary scholarship DCR-004-3.06/21 and CNPq (National Council for Scientific and Technological Development, Brazil) for scholarship 300883/2021-8. This article is in part a result of the projects APQ-0210-3.06/19 and APQ-0726-5.07/21 from FACEPE. Furthermore, M.F.D.S. would also like to thank CETENE/MCTI (Centro de Tecnologias Estratégicas do Nordeste/Ministério da Ciência, Tecnologia e Inovação) and CNPq, grant number 301123/2023-3.

Conflicts of Interest: The authors declare no conflict of interest.

References

1. Eixenberger, D.; Kumar, A.; Klinger, S.; Scharnagl, N.; Dawood, A.W.H.; Liese, A. Polymer-grafted 3D-printed material for enzyme immobilization—designing a smart enzyme carrier. *Catalysts* **2023**, *13*, 1130. [CrossRef]
2. de Oliveira, R.L.; dos Santos, V.L.V.; da Silva, M.F.; Porto, T.S. Kinetic/thermodynamic study of immobilized β-fructofuranosidase from *Aspergillus tamarii* URM4634 in chitosan beads and application on invert sugar production in packed bed reactor. *Food Res. Int.* **2020**, *137*, 109730. [CrossRef] [PubMed]
3. Silva, J.D.C.; de França, P.R.L.; Converti, A.; Porto, T.S. Pectin hydrolysis in cashew apple juice by *Aspergillus aculeatus* URM4953 polygalacturonase covalently-immobilized on calcium alginate beads: A kinetic and thermodynamic study. *Int. J. Biol. Macromol.* **2019**, *126*, 820–827. [CrossRef] [PubMed]

4. Da Silva, O.S.; de Oliveira, R.L.; Silva, J.D.C.; Converti, A.; Porto, T.S. Thermodynamic investigation of an alkaline protease from *Aspergillus tamarii* URM4634: A comparative approach between crude extract and purified enzyme. *Int. J. Biol. Macromol.* **2018**, *109*, 1039–1044. [CrossRef]
5. Sayed Mostafa, H. Production of low-tannin *Hibiscus sabdariffa* tea through D-optimal design optimization of the preparation conditions and the catalytic action of new tannase. *Food Chem. X.* **2023**, *17*, 100562. [CrossRef] [PubMed]
6. Mansor, A.; Samat, N.; Mat Amin, N.; Syaril Ramli, M.; Siva, R. Chapter. Microbial tannase production from agro-industrial byproducts for industrial applications. In *Microbial Bioprocessing of Agri-Food Wastes. Industrial Enzymes*, 1st ed.; Molina, G., Usmani, Z., Sharma, M., Benhida, R., Kuhad, R.C., Gupta, V.K., Eds.; CRC Press: Boca Raton, FL, USA, 2023; p. 40, ISBN 9781003341017.
7. Benucci, I.; Lombardelli, C.; Esti, M. Innovative continuous biocatalytic system based on immobilized tannase: Possible prospects for the haze-active phenols hydrolysis in brewing industry. *Eur. Food Res. Technol.* **2023**. [CrossRef]
8. Kumar, M.; Mehra, R.; Yogi, R.; Singh, N.; Salar, R.K.; Saxena, G.; Rustagi, S. A novel tannase from *Klebsiella pneumoniae* KP715242 reduces haze and improves the quality of fruit juice and beverages through detannification. *Front. Sustain. Food Syst.* **2023**, *7*, 1173611. [CrossRef]
9. Song, L.; Wang, X.-C.; Feng, Z.-Q.; Guo, Y.-F.; Meng, G.-Q.; Wang, H.-Y. Biotransformation of gallate esters by a pH-stable tannase of mangrove-derived yeast *Debaryomyces hansenii*. *Front. Mol. Biosci.* **2023**, *10*, 1211621. [CrossRef] [PubMed]
10. Ristinmaa, A.S.; Coleman, T.; Cesar, L.; Weinmann, A.L.; Mazurkewich, S.; Branden, G.; Hasani, M.; Larsbrink, J. Structural diversity and substrate preferences of three tannase enzymes encoded by the anaerobic bacterium *Clostridium butyricum*. *J. Biol. Chem.* **2022**, *298*, 101758. [CrossRef] [PubMed]
11. Abdel-Naby, M.A.; El-Tanash, A.B.; Sherief, A.D.A. Structural characterization, catalytic, kinetic and thermodynamic properties of *Aspergillus oryzae* tannase. *Int. J. Biol. Macromol.* **2016**, *92*, 803–811. [CrossRef] [PubMed]
12. Xie, J.; Zhang, Y.; Simpson, B. Food enzymes immobilization: Novel carriers, techniques and applications. *Curr. Opin. Food Sci.* **2022**, *43*, 27–35. [CrossRef]
13. Maghraby, Y.R.; El-Shabasy, R.M.; Ibrahim, A.H.; El-Said Azzazy, H.M. Enzyme immobilization technologies and industrial applications. *ACS Omega* **2023**, *8*, 5184–5196. [CrossRef] [PubMed]
14. Silva, J.D.C.; de França, P.R.L.; Converti, A.; Porto, T.S. Kinetic and thermodynamic characterization of a novel *Aspergillus aculeatus* URM4953 polygalacturonase. Comparison of free and calcium alginate-immobilized enzyme. *Process Biochem.* **2018**, *74*, 61–70. [CrossRef]
15. Miguel Júnior, J.; Mattos, F.R.; Costa, G.R.; Zurlo, A.B.R.; Fernandez-Lafuente, R.; Mendes, A.A. Improved catalytic performance of Lipase Eversa® Transform 2.0 via immobilization for the sustainable production of flavor esters—Adsorption process and environmental assessment studies. *Catalysts* **2022**, *12*, 1412. [CrossRef]
16. Valls-Chivas, A.; Gómez, J.; Garcia-Peiro, J.I.; Hornos, F.; Hueso, J.L. Enzyme–iron oxide nanoassemblies: A review of immobilization and biocatalytic applications. *Catalysts* **2023**, *13*, 980. [CrossRef]
17. Larosa, C.; Salerno, M.; de Lima, J.S.; Meri, R.M.; da Silva, M.F.; de Carvalho, L.B.; Converti, A. Characterisation of bare and tannase-loaded calcium alginate beads by microscopic, thermogravimetric, FTIR and XRD analyses. *Int. J. Biol. Macromol.* **2018**, *115*, 900–906. [CrossRef]
18. Intisar, A.; Hedar, H.; Sharif, A.; Ahmed, E.; Hussain, N.; Hadibarata, H.; Ali Shariati, M.; Smaoui, S. Chapter 21–Enzyme immobilization on alginate biopolymer for biotechnological applications. In *Microbial Biomolecules. Emerging Approach in Agriculture, Pharmaceuticals and Environment Management. Developments in Applied Microbiology and Biotechnology*; Elsevier: Amsterdam, The Netherlands, 2023; pp. 471–488, ISBN 978-0-323-99476-7. [CrossRef]
19. de Lima, J.S.; Cabrera, M.P.; Casazza, A.A.; da Silva, M.F.; Perego, P.; de Carvalho, L.B., Jr.; Converti, A. Immobilization of *Aspergillus ficuum* tannase in calcium alginate beads and its application in the treatment of boldo (*Peumus boldus*) tea. *Int. J. Biol. Macromol.* **2018**, *118*, 1989–1994. [CrossRef]
20. Cabrera, M.P.; da Fonseca, T.F.; de Souza, R.V.B.; de Assis, C.R.D.; Marcatoma, J.Q.; Maciel, J.D.C.; Neri, D.F.M.; Soria, F.; de Carvalho, L.B., Jr. Polyaniline-coated magnetic diatomite nanoparticles as a matrix for immobilizing enzymes. *Appl. Surf. Sci.* **2018**, *457*, 21–29. [CrossRef]
21. de Lima, J.S.; Cabrera, M.P.; Motta, C.M.D.S.; Converti, A.; Carvalho, L.B., Jr. Hydrolysis of tannins by tannase immobilized onto magnetic diatomaceous earth nanoparticles coated with polyaniline. *Food Res. Int.* **2018**, *107*, 470–476. [CrossRef]
22. Gao, X.; Pan, H.; Tian, S.; Su, L.; Hu, Z.; Qiao, C.; Liu, Q.; Zhou, C. Co-immobilization of bienzyme HRP/GO_x on highly stable hierarchically porous MOF with enhanced catalytic activity and stability: Kinetic and thermodynamic studies. *J. Environ. Chem. Eng.* **2023**, *11*, 110684. [CrossRef]
23. Wahba, M.I.; Saleh, S.A.A.; Mostafa, F.A.; Abdel Wahab, W.A. Immobilization impact of GEG-Alg-SPI as a carrier for *Aspergillus niger* MK981235 inulinase: Kinetics, thermodynamics, and application. *Bioresour. Technol. Rep.* **2022**, *18*, 101099. [CrossRef]
24. De Oliveira, R.L.; da Silva, M.F.; da Silva, S.P.; Cavalcanti, J.V.F.L.; Converti, A.; Porto, T.S. Immobilization of a commercial *Aspergillus aculeatus* enzyme preparation with fructosyltransferase activity in chitosan beads: A kinetic/thermodynamic study and fructo-oligosaccharides continuous production in enzymatic reactor. *Food Bioprod. Process.* **2020**, *122*, 169–182. [CrossRef]
25. De Oliveira, R.L.; da Silva, S.P.; Converti, A.; Porto, T.S. Production, biochemical characterization, and kinetic/thermodynamic study of inulinase from *Aspergillus terreus* URM4658. *Molecules* **2022**, *27*, 6418. [CrossRef] [PubMed]

26. De Oliveira, R.L.; Claudino, E.S.; Converti, A.; Porto, T.S. Use of a sequential fermentation method for the production of *Aspergillus tamarii* URM4634 protease and a kinetic/thermodynamic study of the enzyme. *Catalysts* **2021**, *11*, 963. [CrossRef]
27. Fernandes, L.M.G.; Carneiro-da-Cunha, M.N.; Silva, J.D.C.; Porto, A.L.F.; Porto, T.S. Purification and characterization of a novel *Aspergillus heteromorphus* URM 0269 protease extracted by aqueous two-phase systems PEG/citrate. *J. Mol. Liq.* **2020**, *317*, 113957. [CrossRef]
28. Boudrant, J.; Woodley, J.M.; Fernandez-Lafuente, R. Parameters necessary to define an immobilized enzyme preparation. *Process Biochem.* **2020**, *90*, 66–80. [CrossRef]
29. Abellanas-Perez, P.; Carballares, D.; Fernandez-Lafuente, R.; Rocha-Martin, J. Glutaraldehyde modification of lipases immobilized on octyl agarose beads: Roles of the support enzyme loading and chemical amination of the enzyme on the final enzyme features. *Int. J. Biol. Macromol.* **2023**, *248*, 125853. [CrossRef] [PubMed]
30. Heidtmann, R.B.; Duarte, S.H.; de Pereira, L.P.; Braga, A.R.C.; Kalil, S.J. Caracterização cinética e termodinâmica de β-galactosidase de *Kluyveromyces marxianus* CCT 7082 fracionada com sulfato de amônio. *Braz. J. Food Technol.* **2012**, *15*, 41–49. [CrossRef]
31. Khatun, S.; Riyazuddeen; Yasmeen, S. Unraveling the thermodynamics, enzyme activity and denaturation studies of triprolidine hydrochloride binding with model transport protein. *J. Mol. Liq.* **2021**, *337*, 116569. [CrossRef]
32. Rodríguez-López, J.N.; Fenoll, L.G.; Tudela, J.; Devece, C.; Sánchez-Hernández, D.; de los Reyes, E.; García-Cánovas, F. Thermal Inactivation of Mushroom Polyphenoloxidase Employing 2450 MHz Microwave Radiation. *J. Agric. Food Chem.* **1999**, *47*, 3028–3035. [CrossRef]
33. Bradford, M.M. A rapid and sensitive method for the quantitation of microgram quantities of protein utilizing the principle of protein-dye binding. *Anal. Biochem.* **1976**, *72*, 248–254. [CrossRef] [PubMed]
34. Pinto, G.A.S.; Couri, S.; Gonçalves, E.B. Replacement of methanol by ethanol on gallic acid determination by rhodanine and its impacts on the tannase assay. *Electron. J. Environ. Agric. Food Chem.* **2006**, *5*, 1560–1568.
35. Da Silva, O.S.; Silva, J.D.C.; de Almeida, E.M.; Sousa, F.; Gonçalves, O.S.L.; Sarmento, B.; Neves-Petersen, M.T.; Porto, T.S. Biophysical, photochemical and biochemical characterization of a protease from *Aspergillus tamarii* URM4634. *Int. J. Biol. Macromol.* **2018**, *118*, 1655–1666. [CrossRef]
36. Michel, D. Simply conceiving the Arrhenius law and absolute kinetic constants using the geometric distribution. *Phys. A Stat. Mech. Appl.* **2013**, *392*, 4258–4264. [CrossRef]
37. Converti, A.; Pessoa, A., Jr.; Silva, J.D.C.; de Oliveira, R.L.; Porto, T.S. Thermodynamics applied to biomolecules. In *Pharmaceutical Biotechnology: A Focus on Industrial Application*; Pessoa, A., Jr., Vitolo, M., Long, P.F., Eds.; CRC Press: Boca Raton, FL, USA, 2021; Volume 1, pp. 29–42, ISBN 9781000399844.
38. Ortega, N.; de Diego, S.; Perez-Mateos, M.; Busto, M.D. Kinetic properties and thermal behaviour of polygalacturonase used in fruit juice clarification. *Food Chem.* **2004**, *88*, 209–217. [CrossRef]